

High-speed imaging of Strombolian explosions: The ejection velocity of pyroclasts

J. Taddeucci,¹ P. Scarlato,¹ A. Capponi,² E. Del Bello,¹ C. Cimarelli,³ D. M. Palladino,² and U. Kueppers³

Received 18 November 2011; revised 12 December 2011; accepted 12 December 2011; published 18 January 2012.

[1] Explosive volcanic eruptions are defined as the violent ejection of gas and hot fragments from a vent in the Earth's crust. Knowledge of ejection velocity is crucial for understanding and modeling relevant physical processes of an eruption, and yet direct measurements are still a difficult task with largely variable results. Here we apply pioneering high-speed imaging to measure the ejection velocity of pyroclasts from Strombolian explosive eruptions with an unparalleled temporal resolution. Measured supersonic velocities, up to 405 m/s, are twice higher than previously reported for such eruptions. Individual Strombolian explosions include multiple, sub-second-lasting ejection pulses characterized by an exponential decay of velocity. When fitted with an empirical model from shock-tube experiments literature, this decay allows constraining the length of the pressurized gas pockets responsible for the ejection pulses. These results directly impact eruption modeling and related hazard assessment, as well as the interpretation of geophysical signals from monitoring networks. **Citation:** Taddeucci, J., P. Scarlato, A. Capponi, E. Del Bello, C. Cimarelli, D. M. Palladino, and U. Kueppers (2012), High-speed imaging of Strombolian explosions: The ejection velocity of pyroclasts, *Geophys. Res. Lett.*, 39, L02301, doi:10.1029/2011GL050404.

1. Introduction

[2] Explosive volcanic eruptions eject a mixture of hot gas and fragments (pyroclasts) out of a vent and into the Earth's atmosphere or hydrosphere. The ejection velocity of pyroclasts is one of the most important parameters of an eruption, being directly related to the driving pressure and controlling the mode and range of pyroclast dispersal. Despite this crucial role, direct measurement of pyroclast ejection velocity is still a difficult task, and available results vary largely depending on analytical technique and eruption style.

[3] Given their intrinsically hazardous nature, the in-situ parameterization of explosive eruptions is more advanced at the lower end of the eruptive intensity spectrum, where activity

is relatively more accessible. Strombolian eruption of low-viscosity mafic magma is the least intense and most frequent type of explosive volcanic activity on Earth [Houghton and Gonnermann, 2008]. Typical Strombolian eruptions consist of recurrent, seconds-lasting explosions that eject centimeter- to meter-sized molten fragments to heights up to a few hundred of meters above the volcanic vent. The impulsive character of this kind of activity has long been attributed to the bursting of individual, large (meter-sized) gas bubbles at the surface of a stagnant magma column residing in the conduit [e.g., Vergnolle and Mangan, 2000], as also supported by geophysical evidence [e.g., Harris and Ripepe, 2007].

[4] At Stromboli (Italy), the type locality for Strombolian activity, pyroclast ejection velocity was first measured by means of photoballistic techniques [Chouet et al., 1974; Blackburn et al., 1976; Ripepe et al., 1993], and more recently by acoustic Doppler sounder [Weill et al., 1992], Doppler radar [Hort et al., 2003; Gerst et al., 2008; Scharff et al., 2008], and FLIR [Patrick et al., 2007] (Table 1). In addition, ejection velocity has been inferred from the range of ballistically emplaced bombs and bubble oscillation models [e.g., Vergnolle and Brandeis, 1996]. Ejection velocity from Strombolian activity has served as an input parameter both for modeling the initial pressure and decompression rate of the gas phase driving explosions [e.g., Wilson, 1980], and for hazard assessment, e.g., calculating the range of ballistic bombs [Mastin, 1995, 2001] or the development of volcanic plumes [Patrick, 2007].

2. Video Acquisition and Processing

[5] High-speed videos of eruptive activity at Stromboli were acquired during several field campaigns since 2005. In this paper we focus on six videos of ash-free explosions from two vents in the south-west vent area (hereafter SW1 and SW2, Figure 1) acquired on 17 June and 27 October 2009. We used a monochrome NAC HotShot 512 SC high-speed camera, operating for up to 32.6 s at 500 frames per second. The circular memory buffer of the camera allows recording before hand-triggering, thus capturing the very onset of each explosion. The 512 × 512 pixel resolution C-MOS sensor of the camera is sensitive to visible and partly to near-infrared radiation, allowing hot pyroclasts to be easily recognized from colder ones by their brighter tone in the videos. Video resolution is 0.018 (SW2) and 0.021 (SW1) meters per pixel, as calculated from the camera angle of view and the camera-crater distance and inclination, measured with a laser telemeter.

[6] Ejection velocity was measured by using the ImageJ freeware software and the MTrackJ plug-in [Abramoff

¹Department of Seismology and Tectonophysics, Istituto Nazionale di Geofisica e Vulcanologia, Rome, Italy.

²Dipartimento di Scienze della Terra, Università di Roma "La Sapienza," Rome, Italy.

³Department of Earth and Environmental Sciences, Ludwig-Maximilians-University, Munich, Germany.

Table 1. Ejection Velocity of Pyroclasts During Strombolian Activity at Stromboli Volcano

Reference ^a	Literature Measurements		Method
	V max (m/s)	V mean (m/s)	
1	70	26	particle streak-length on film
2	65	56	film tracking
3	80	42	acoustic Doppler sounder
4		22	average particle tracking
5	70		Doppler radar
6	101	34	plume tracking by FLIR
7		17	Doppler radar

Explosion	This Work	
	V max (m/s)	V mean (m/s)
SW1_1	172	38
SW1_2	259	53
SW1_3	230	48
SW2_1	405	136
SW2_2	367	149
SW2_3	370	98

^aReferences: 1, Chouet et al. [1974]; 2, Blackburn et al. [1976]; 3, Weill et al. [1992]; 4, Ripepe et al. [1993]; 5, Hort et al. [2003]; 6, Patrick et al. [2007]; 7, Scharff et al. [2008].

et al., 2004], tracking for 5–10 frames the trajectory of centimeter-sized pyroclasts exiting the vent. A new trajectory was initiated every 2–4 frames, focusing on the fastest pyroclasts. For each trajectory, we calculated the average velocity and standard deviation over the measured frames. Measured velocities are conservative values for two reasons. First, the two-dimensional view does not account for velocity components towards or away from the camera. Thus we corrected all measured velocities by dividing them by the sine of $90^\circ - \alpha$ ($\alpha = 32^\circ$, the camera tilt angle below horizontal, Figure 1). This correction provides actual velocities for those clasts that are ejected vertically (90°), i.e., during the fastest, well-collimated, initial phases of explosive events (as confirmed by INGV surveillance videos shot perpendicularly to our line of view), while velocity is overestimated by <20% for clasts ejected at 90° – 160° (away from the camera), and underestimated for all other ejection angles. Second, the velocity is averaged over several frames during which pyroclasts are sometimes observed to decelerate. We tracked pyroclasts for a number of frames large enough to reduce tracking errors but small enough to minimize pyroclast deceleration.

[7] To obtain an independent measure of the ejection velocity, we acquired some videos with an intentionally long

shutter exposure time, then measuring on one frame the length of the streak left by pyroclasts, which is proportional to the ejection velocity. Streak-length and tracking velocity values of test pyroclasts agree within 10%, whereas streak-length velocity has larger errors, its applicability



Figure 1. (top) Southward view of the field setup for the high-speed filming experiments at Stromboli volcano. The camera, located at Pizzo Sopra la Fossa and tilted downward by 32° , looks at the 320- and 290-m away SW1 and SW2 vents. Representative still-frames of (middle) a meter-sized bubble bursting at the surface of SW1 vent and (bottom) a well-collimated ejection jet at the beginning of an explosion at SW2 vent. Incandescent pyroclasts are in white, clearly distinguishable from darker (colder) surroundings.

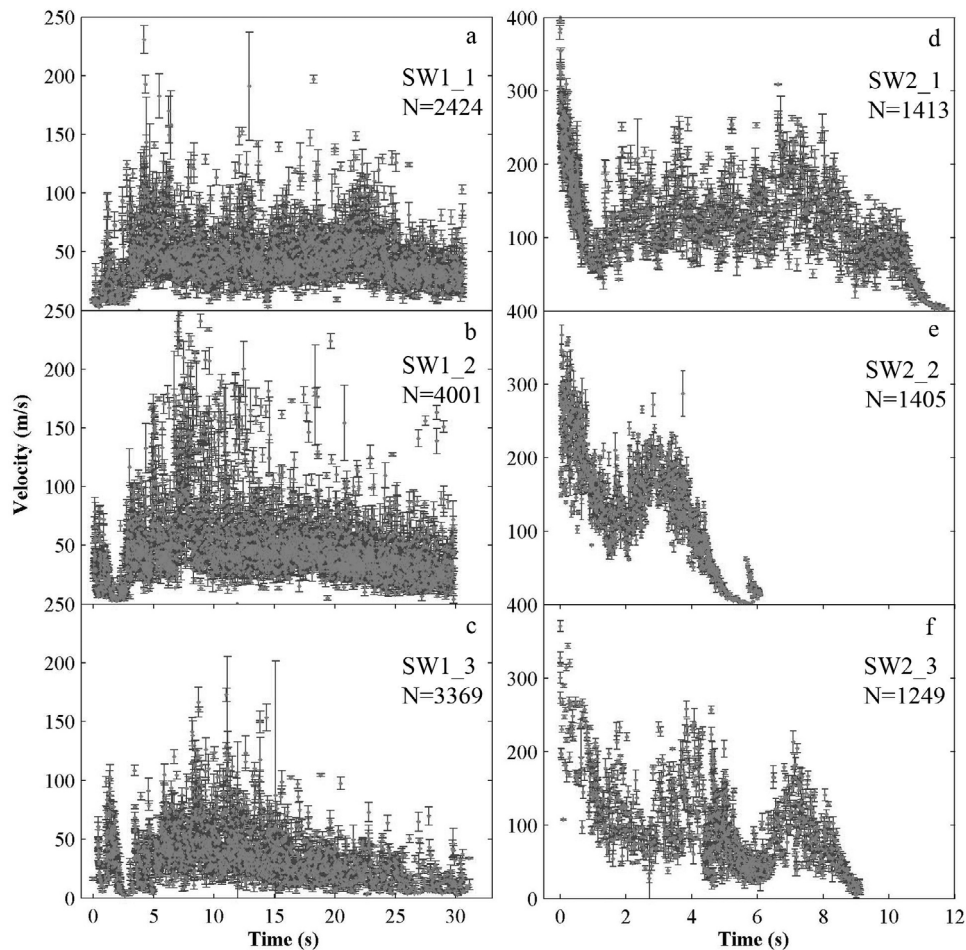


Figure 2. Ejection velocity of pyroclasts over time for events (a, b, c) SW1_1-3 and (d, e, f) SW2_1-3 (N = number of measured pyroclasts). Each point represents the velocity of a single centimeter-sized pyroclast, corrected for the tilt angle of the camera, and averaged over 5–10 frames (error bar is $\pm 1\sigma$). Time is normalized to the ejection time of the first erupted pyroclast, with error bar (i.e., the error of the camera internal clock) being smaller than symbol. Note the different time and velocity scales for the two vents.

being more limited in terms of range of ejection velocity and lighting conditions.

3. Results

[8] High-speed videos show that explosive events at SW1 are preceded by several discrete cycles of inflation/deflation of the crater floor (Movie 1¹), followed by the bursting of meter-sized bubbles (Movie 1, part 1), until pyroclast ejection becomes almost continuous, including meter-sized spatter bombs (Figure 1 and Movie 1, part 2). In the videos, explosions at SW2 are often preceded by a shock wave, followed by the appearance of a well-collimated jet of fast, centimeter-sized pyroclasts that gradually decrease in velocity and increase in size and abundance (Figure 1 and Movie 2, part 1). The explosion then proceeds as discrete pyroclast ejection pulses (Movie 2, parts 2 and 3), with occasional ejection of meter-sized bombs, sometimes fragmenting in-flight, and end with a gradual decrease in the number, velocity, and size of pyroclasts. Both SW1 and SW2 feature vent diameters of ~ 2.5 m.

[9] The duration and velocity history of explosions differ at the two vents (Figure 2). Explosions last >32.6 s (the maximum recording time of the camera) at SW1 and 6–13 s, set unambiguously by the first- and last-observed ejected pyroclast, at SW2. SW1 events are characterized by a baseline velocity <50 m/s, and feature tens of velocity peaks with highly variable, but usually <250 m/s, velocities. Initial, short-duration, low-velocity peaks are clearly separated, while subsequent ones occur more frequently so that their individual decay trends blend together. Although the end of the explosion is not recorded, a gradual decrease in velocity over tens of seconds is evident. Conversely, explosions at SW2 invariably start with one dominant peak of fast (always supersonic in ambient air and up to 405 m/s) pyroclasts, followed by rapid velocity decay with occasional fluctuations. Then a few evident velocity fluctuations (100–200 m/s) occur, and explosions end with a well-defined coda of decreasing pyroclast velocity.

[10] In all events, clearly defined velocity peaks last ~ 0.2 –3 s and display a non-linear decay of velocity over time. Visually, these peaks correspond to discrete, well-collimated pyroclast ejection pulses throughout the explosions, occasionally directly related to the bursting of meter-sized

¹Animations are available in the HTML.

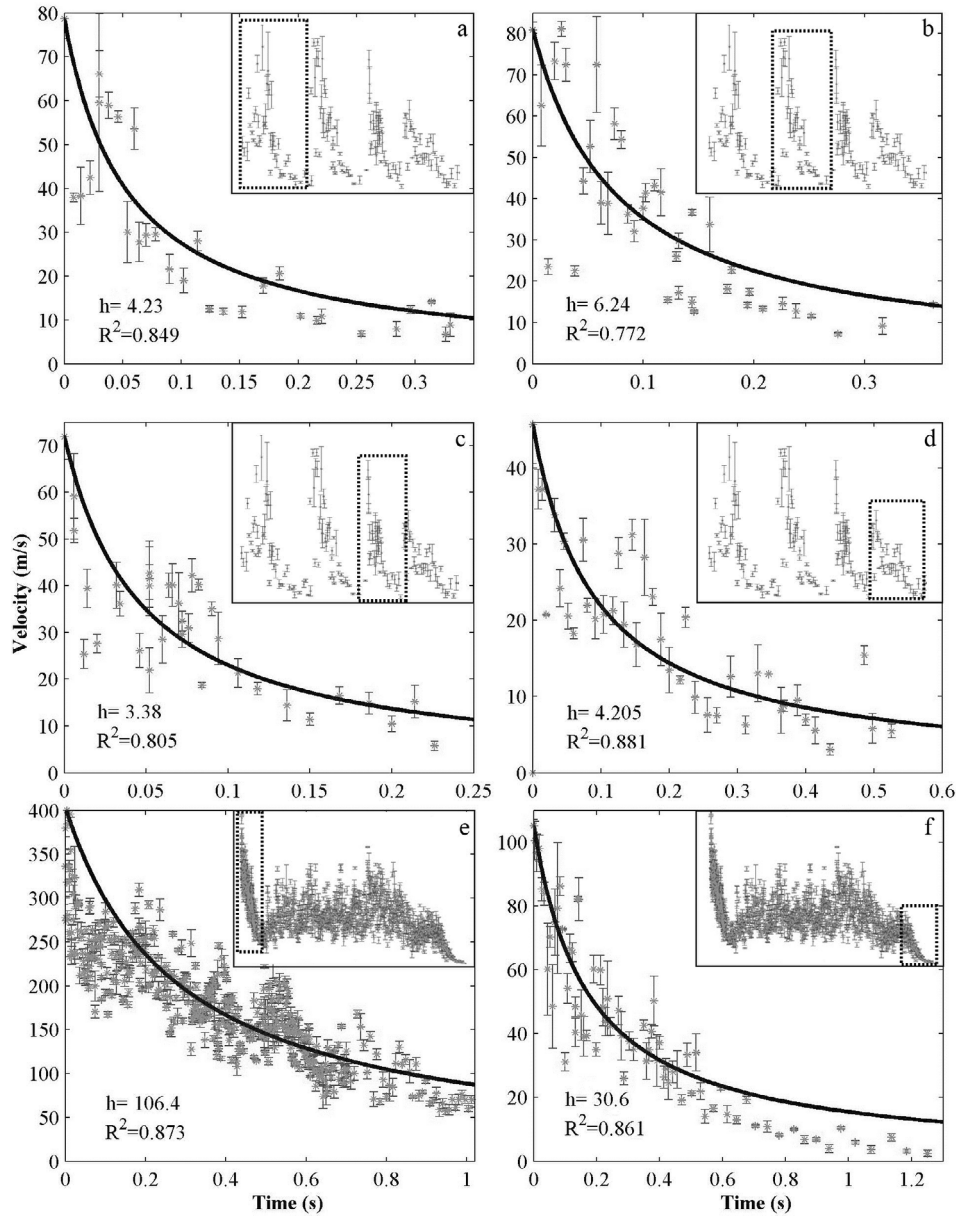


Figure 3. Fitting of the *Alatorre-Ibargüengoitia et al.* [2010] empirical equation (black line) to (a–d) the four small pulses in the first 3 s of event SW1_2 (dashed boxes in insets) and to the ejection pulses at the (e) beginning and (f) end of event SW2_1. The resulting maximum bursting length (h , distance in meters from the base of the pressurized gas pocket to the camera viewpoint at the vent) is reported together with the coefficient of determination of the fit (R^2).

bubbles at the surface of SW1. The velocity decay trend of these peaks is reasonably well approximated by the empirical relationship found in shock-tube experiments by *Alatorre-Ibargüengoitia et al.* [2010, 2011] (Figure 3), where a mixture of high-pressure gas and particles is suddenly released into an ambient-pressure chamber:

$$v_p = \frac{v_{\max}}{1 + \frac{v_{\max}}{h} t}, \quad (1)$$

where v_p is particle velocity $f(t)$, $t = 0$ at the time when the first particle is observed, v_{\max} is the maximum ejection velocity, and h corresponds to the vertical distance from the base of the pressurized tube to the recording high-speed camera.

[11] The application of equation (1) (Figure 3) to the initial ejection pulses from SW1 provides a measure of the maximum length at bursting (i.e., the distance from the base of the pressurized gas pocket to the camera viewpoint) of 3–6 m, consistent with the visually observed size of bursting bubbles (Movie 1). The application to the dominant pulses at the onset of SW2 explosions, instead, provides a maximum bursting length $h \sim 100$ m, while velocity decay trends at the explosion coda are related to gas pockets at least 30 m in length.

4. Discussion and Conclusions

[12] The maximum and average high-speed video-derived ejection velocities are at least a factor of four higher than

Stromboli literature (Table 1) and a factor of two higher than more recent measurements by Doppler radar (order of 200 m/s for the vertical component, M. Hort, personal communication, 2011). Likely, the high spatial and temporal resolution of the high-speed videos allows capturing small and fast pyroclasts invisible to other techniques. For instance, the few, supersonic pyroclasts ejected in the first 0.5 s of SW2 explosions can be measured only by filming at high-frequency with a circular memory buffer (unless continuously recording).

[13] Maximum block launch heights <200 m (derived from surveillance camera) suggest that the filmed explosions were not particularly energetic. At Stromboli and other volcanoes, supersonic velocity values are usually only associated with lava fountain, Vulcanian and hydromagmatic eruptions. Such eruptions are orders of magnitude higher in intensity than Strombolian ones, with estimated explosion pressures of tens of bars or more [e.g., Mastin, 1995; Ripepe and Harris, 2008], i.e., remarkably higher than theoretical and field inferences for persistent activity at Stromboli [Blackburn et al., 1976; Vergnolle and Brandeis, 1996; Ripepe and Marchetti, 2002]. This apparent discrepancy is due to the fact that velocity (and hence pressure) peaks are not concomitant to the ejection of large bombs, which, conversely, appear in the high-speed videos during low-velocity phases. Mastin [1995], modeling gas and steam-blast eruptions, concludes that: 1) most solid material is expelled when velocity is low; and 2) velocity observations made on large blocks may be less than the average for the gas-pyroclast mixture. Our high-speed analysis confirms the above conclusions and expands their validity to Strombolian-type eruptions. Perhaps more importantly, it suggests that, for Strombolian eruptions, caution must be used in calculating the ejection velocity and range of ballistic bombs from independent peak pressure estimates (e.g., by acoustic or ground deformation information) and vice versa.

[14] Velocity fluctuations during individual Strombolian explosions have been previously reported and interpreted either as “organ pipe resonance” [Chouet et al., 1974], or as the bursting of several discrete bubbles [Ripepe et al., 1993; Harris and Ripepe, 2007; Scharff et al., 2008]. Velocity pulses may also reflect post-fragmentation pressure fluctuations in the gas-particle mixture rising in the conduit [Cagnoli et al., 2002; Darteville and Valentine, 2007].

[15] The observed trends of velocity decay in individual ejection pulses, analogous to shock-tube experiments [Alatorre-Ibargüengoitia et al., 2010], corroborate the hypothesis that pulses originate from discrete events of pressure release. Also, the consistency of the observed sizes of bursting bubbles from SW1 with estimated maximum length of gas pockets supports the applicability of equation (1) to Strombolian explosions and possibly other eruptions with similar velocity decay trends [e.g., Donnadieu et al., 2005]. Our videos provide clear evidence that multiple ejection pulses at SW1 are directly related to the burst of individual bubbles at the vent. In this regard, lower-velocity, longer-lasting explosions at SW1 seem to represent the continuous bursting of multiple, meter-sized bubbles ascending in the conduit, with a gradual decrease in the ejection velocity mirroring decreasing bubble pressure. Quasi-steady state conditions at the vent require that bubble ascent and bursting rates be comparable. On the other hand, faster and shorter explosions at SW2 appear to start with the bursting of a single, very long

(~100 m; Figure 3) and more pressurized gas pocket, or rather slug, followed by fast refill of the conduit and repeated bursts, ending with a smaller pocket (~30 m) burst that produces the ejection coda. Accelerated rise of underlying slugs and/or enhanced vesiculation resulting from sudden decompression, may contribute to the fast refill of the conduit. Second-order velocity fluctuations during the dominant ejection pulses (Figure 3) would likely reflect, rather than individual bursts, more complex sources of pressure fluctuations. Besides a possible origin within the ascending gas-pyroclast mixture, we suggest that pressure fluctuations may result from transient gas pockets formed by the repeated collapse of the liquid film lining conduit walls during the bursting of long slugs (reminiscent of churn flow conditions). Sustained release of small gas pockets at SW1 and accumulation and release of large pockets at SW2 could mirror conduit geometry in the branching zone.

[16] In conclusion, high-speed imaging provides an innovative tool to investigate and parameterize Strombolian eruptions. Novel information on ejection velocity and bursting length will eventually impact: i) determination of the source parameters and temporal dynamics of the explosions; ii) interpreting geophysical signals acquired by monitoring networks; and iii) assessing and mitigating the hazard related to ballistic volcanic bombs that threaten visitors at Stromboli and other tourists, but nevertheless risky, volcanoes.

[17] **Acknowledgments.** We thank C. Acerra, D. Andronico, L. D’Auria, A. Davila, F. Di Traglia, M. Mari, S. Mueller, M. Orazi, S. Rao, C. Salvaterra, and S. Zaia for invaluable field and technical support; funding from the INGV-DPC “V2” and “Paroxysm”, FIRB-MIUR “Research and Development of New Technologies for Protection and Defense of Territory from Natural Risks”, and FP7-PEOPLE-IEF-2008 – 235328 Projects.

[18] The Editor thanks Larry Mastin and Michelle Coombs for their assistance in evaluating this paper.

References

- Abramoff, M. D., P. J. Magelhaes, and S. J. Ram (2004), Image processing with ImageJ, *Biophotonics Int.*, *11*, 36–42.
- Alatorre-Ibargüengoitia, M. A., B. Scheu, D. B. Dingwell, H. Delgado-Granados, and J. Taddeucci (2010), Energy consumption by magmatic fragmentation and pyroclast ejection during Vulcanian eruptions, *Earth Planet. Sci. Lett.*, *291*, 60–69, doi:10.1016/j.epsl.2009.12.051.
- Alatorre-Ibargüengoitia, M. A., B. Scheu, and D. B. Dingwell (2011), Influence of the fragmentation process on the dynamics of Vulcanian eruptions: An experimental approach, *Earth Planet. Sci. Lett.*, *302*, 51–59, doi:10.1016/j.epsl.2010.11.045.
- Blackburn, E. A., L. Wilson, and R. S. J. Sparks (1976), Mechanism and dynamics of Strombolian activity, *J. Geol. Soc.*, *132*, 429–440, doi:10.1144/gsjgs.132.4.0429.
- Cagnoli, B., A. Barmin, O. Melnik, and R. S. J. Sparks (2002), Depressurization of fine powders in a shock tube and dynamics of fragmented magma in volcanic conduits, *Earth Planet. Sci. Lett.*, *204*, 101–113, doi:10.1016/S0012-821X(02)00952-4.
- Chouet, B., N. Hamisevicz, and T. McGetchin (1974), Photoballistics of volcanic jet activity at Stromboli, Italy, *J. Geophys. Res.*, *79*, 4961–4976, doi:10.1029/JB079i032p04961.
- Darteville, S., and G. A. Valentine (2007), Transient multiphase processes during the explosive eruption of basalt through a geothermal borehole (Námafjall, Iceland, 1977) and implications for natural volcanic flows, *Earth Planet. Sci. Lett.*, *262*, 363–384, doi:10.1016/j.epsl.2007.07.053.
- Donnadieu, F., G. Dubosclard, R. Cordesses, T. H. Druitt, C. Hervier, J. Kornprobst, J.-F. Lénat, P. Allard, and M. Coltelli (2005), Remotely monitoring volcanic activity with ground-based Doppler radar, *Eos Trans. AGU*, *86*, 201, doi:10.1029/2005EO210001.
- Gerst, A., M. Hort, P. R. Kyle, and M. Voge (2008), 4D velocity of Strombolian eruptions and man-made explosions derived from multiple Doppler radar instruments, *J. Volcanol. Geotherm. Res.*, *177*(3), 648–660, doi:10.1016/j.jvolgeores.2008.05.022.
- Harris, A., and M. Ripepe (2007), Synergy of multiple geophysical approaches to unravel explosive eruption conduit and source dynamics—

- A case study from Stromboli, *Chem. Erde*, 67, 1–35, doi:10.1016/j.chemer.2007.01.003.
- Hort, M., R. Seyfried, and M. Voegelé (2003), Radar Doppler velocimetry of volcanic eruptions: Theoretical considerations and quantitative documentation of changes in eruptive behaviour at Stromboli volcano, Italy, *Geophys. J. Int.*, 154, 515–532, doi:10.1046/j.1365-246X.2003.01982.x.
- Houghton, B. F., and H. M. Gonnermann (2008), Basaltic explosive volcanism: Constraints from deposits and models, *Chem. Erde*, 68(2), 117–140, doi:10.1016/j.chemer.2008.04.002.
- Mastin, L. G. (1995), Thermodynamics of gas and steam-blast eruptions, *Bull. Volcanol.*, 57, 85–98.
- Mastin, L. G. (2001), A simple calculator of ballistic trajectories for blocks ejected during volcanic eruptions, *U.S. Geol. Surv. Open File Rep.*, 01–45, U.S. Geological Survey, Reston, Virginia.
- Patrick, M. R. (2007), Dynamics of Strombolian ash plumes from thermal video: Motion, morphology, and air entrainment, *J. Geophys. Res.*, 112, B06202, doi:10.1029/2006JB004387.
- Patrick, M. R., A. Harris, M. Ripepe, J. Dehn, D. A. Rothery, and S. Calvari (2007), Strombolian explosive styles and source conditions: Insights from thermal (FLIR) video, *Bull. Volcanol.*, 69, 769–784, doi:10.1007/s00445-006-0107-0.
- Ripepe, M., and A. J. L. Harris (2008), Dynamics of the 5 April 2003 explosive paroxysm observed at Stromboli by a near-vent thermal, seismic and infrasonic array, *Geophys. Res. Lett.*, 35, L07306, doi:10.1029/2007GL032533.
- Ripepe, M., and E. Marchetti (2002), Array tracking of infrasonic sources at Stromboli volcano, *Geophys. Res. Lett.*, 29(22), 2076, doi:10.1029/2002GL015452.
- Ripepe, M., M. Rossi, and G. Saccorotti (1993), Image processing of explosive activity at Stromboli, *J. Volcanol. Geotherm. Res.*, 54, 335–351, doi:10.1016/0377-0273(93)90071-X.
- Scharff, L., M. Hort, A. J. L. Harris, M. Ripepe, J. M. Lees, and R. Seyfried (2008) Eruption dynamics of the SW crater of Stromboli volcano, Italy—An interdisciplinary approach, *J. Volcanol. Geotherm. Res.*, 176, 565–570, doi:10.1016/j.jvolgeores.2008.05.008.
- Vergnolle, S., and G. Brandeis (1996), Strombolian explosions: 1. A large bubble breaking at the surface of a lava column as a source of sound, *J. Geophys. Res.*, 101, 20,433–20,447, doi:10.1029/96JB01178.
- Vergnolle, S., and M. Mangan (2000), Hawaiian and Strombolian eruptions, in *Encyclopedia of Volcanoes*, edited by H. Sigurdsson et al., pp. 447–461, Academic, San Diego, Calif.
- Weill, A., G. Brandeis, S. Vergnolle, F. Baudin, J. Bilbille, J. F. Fèvre, B. Piron, and X. Hill (1992), Acoustic sounder measurements of the vertical velocity of volcanic jets at Stromboli volcano, *Geophys. Res. Lett.*, 19, 2357–2360, doi:10.1029/92GL02502.
- Wilson, L. (1980), Relationships between pressure, volatile content and ejecta velocity, *J. Volcanol. Geotherm. Res.*, 8, 297–313, doi:10.1016/0377-0273(80)90110-9.

A. Capponi and D. M. Palladino, Dipartimento di Scienze della Terra, Università di Roma “La Sapienza,” I-00185, Rome, Italy.

C. Cimarelli and U. Kueppers, Department of Earth and Environmental Sciences, Ludwig-Maximilians-University, Theresienstr. 41, D-80333, Munich, Germany.

E. Del Bello, P. Scarlato, and J. Taddeucci, Department of Seismology and Tectonophysics, Istituto Nazionale di Geofisica e Vulcanologia, Via di Vigna Murata 605, I-00143, Rome, Italy. (taddeucci@ingv.it)